


Nargozy Danaev  
Yurii Shokin  
Darkhan Akhmed-Zaki (Eds.)

Communications in Computer and Information Science

549

# Mathematical Modeling of Technological Processes

8th International Conference, CITech 2015  
Almaty, Kazakhstan, September 24–27, 2015  
Proceedings

 Springer

# Communications in Computer and Information Science

549

*Commenced Publication in 2007*

Founding and Former Series Editors:

Alfredo Cuzzocrea, Dominik Ślęzak, and Xiaokang Yang

## Editorial Board

Simone Diniz Junqueira Barbosa

*Pontifical Catholic University of Rio de Janeiro (PUC-Rio),  
Rio de Janeiro, Brazil*

Phoebe Chen

*La Trobe University, Melbourne, Australia*

Xiaoyong Du

*Renmin University of China, Beijing, China*

Joaquim Filipe

*Polytechnic Institute of Setúbal, Setúbal, Portugal*

Orhun Kara

*TÜBİTAK BİLGEM and Middle East Technical University, Ankara, Turkey*

Igor Kotenko

*St. Petersburg Institute for Informatics and Automation of the Russian  
Academy of Sciences, St. Petersburg, Russia*

Ting Liu

*Harbin Institute of Technology (HIT), Harbin, China*

Krishna M. Sivalingam

*Indian Institute of Technology Madras, Chennai, India*

Takashi Washio

*Osaka University, Osaka, Japan*

Nargozy Danaev · Yurii Shokin  
Darkhan Akhmed-Zaki (Eds.)

# Mathematical Modeling of Technological Processes

8th International Conference, CITech 2015  
Almaty, Kazakhstan, September 24–27, 2015  
Proceedings

 Springer

## Contents

Mathematical Modelling of Oil Recovery by Polymer/Surfactant Flooding . . . <i>Nargozy Danaev, Darkhan Akhmed-Zaki, Saltanbek Mukhambetzhonov, and Timur Imankulov</i>	1
Modelling of Evolution Small-Scale Magnetohydrodynamic Turbulence Depending on the Magnetic Viscosity of the Environment . . . . . <i>Aigerim Abdibekova, Bakhytzhon Zhmagulov, and Dauren Zhakebayev</i>	13
Enhancement of the In-Situ Leach Mineral Mining Process by the Hydrodynamic Method . . . . . <i>Karlygash Alibayeva and Aidarkhan Kaltayev</i>	26
Numerical Modeling of Artificial Heart Valve . . . . . <i>Dmitriy Dolgov and Yury Zakharov</i>	33
Numerical Model of Plasma-chemical Etching of Silicon in $CF_4/H_2$ Plasma . . . . . <i>Aleksey Gorobchuk</i>	44
Simulation of Transonic Airfoil Flow Using a Zonal RANS-LES Method . . . <i>Alibek Issakhov, Benedikt Roidl, Matthias Meinke, and Wolfgang Schröder</i>	53
Mathematical Algorithm for Calculation of the Moving Tsunami Wave Height . . . . . <i>Sergey Kabanikhin and Olga Krivorotko</i>	66
Hybrid Evolutionary Approach to Multi-objective Mission Planning for Group of Underwater Robots. . . . . <i>Maksim Kenzin, Igor Bychkov, and Nikolai Maksimkin</i>	73
Theoretical and Numerical Prediction of the Permeability of Fibrous Porous Media . . . . . <i>Aziz Kudaikulov, Christophe Josserand, and Aidarkhan Kaltayev</i>	85
A Study of (m,k)-Methods for Solving Differential-Algebraic Systems of Index 1 . . . . . <i>Alexander I. Levykin and Eugeny A. Novikov</i>	94
Application of Immersed Boundary Method in Modelling of Thrombosis in the Blood Flow. . . . . <i>Saule Maussumbekova and Assel Beketaeva</i>	108

# Modelling of Evolution Small-Scale Magnetohydrodynamic Turbulence Depending on the Magnetic Viscosity of the Environment

Aigerim Abdibekova<sup>1</sup>(✉), Bakhytzhan Zhumagulov<sup>2</sup>,  
and Dauren Zhakebayev<sup>1</sup>(✉)

<sup>1</sup> Al-Farabi Kazakh National University, Al-Farabi ave. 71,  
050040 Almaty, Kazakhstan  
a.aigerim@inbox.ru, daurjaz@mail.ru

<sup>2</sup> National Academy of Engineering of the Republic Kazakhstan,  
Bogenbai Batyr str. 80, 050010 Almaty, Kazakhstan

**Abstract.** The present work is devoted to study of self-excitation of magnetic field and the motion of the conducting fluid at the same time taking into account acting forces. The idea is to specify in the phase space of initial conditions for the velocity field and magnetic field, which satisfy the condition of continuity. Given initial condition with the phase space is translated into physical space using a Fourier transform. The obtained velocity field and magnetic field are used as initial conditions for the filtered MHD equations. Further is solved the unsteady three-dimensional equation of magnetohydrodynamics to simulate homogeneous MHD turbulence decay.

**Keywords:** MHD turbulence · Turbulence · Small-scale · LES

## 1 Introduction

An examination of the homogeneous magnetohydrodynamic turbulence decay process, in spite of the large number of publications in this field, is a relevant task for researchers of several generations. The influence of magnetic field on the conducting fluid is studied in various fields of science and used in an engineering and technology. Therefore, studies of magnetohydrodynamic turbulence decay is an important task in the fields of: forming astrophysical and geophysical phenomena, MHD generators, plasma accelerators and engines. The study of the magnetohydrodynamic (MHD) turbulence process in a small range of change of the Reynolds ( $Re_m$ ) magnetic number can be modeled and experimentally investigated, while the same process remains beyond experimental reach and computational techniques for a broad range of values. Research problems of the magnetic field depending on the electro conductive fluid is divided into three types:

1. An examination of the MHD turbulence at a constant value of the magnetic field.
2. An examination of the self-excitation of magnetic field at a given velocity of the flow.
3. An examination of the self-excitation of magnetic field and the motion of a conducting fluid at the same time taking into account acting forces.

The problem of the magnetic field influence on turbulent flows was first raised by [1], who provided basic equations and an analytical solution for the movement of an electrically conducting fluid. The first numerical study of magnetohydrodynamic turbulence problem of the first type conducted by [2] at the magnetic number  $Re_m \ll 1$ . The numerical experiment of Schumann was the reflection of the idea of [3], who researched a homogeneous isotropic flow influenced by an applied external magnetic field. The modeling outlined in the publications of these scientists is performed using a spectral method, which is used as the basis for presenting a quantitative description of magnetic damping, the emergence of anisotropy, and the dependency of the results on the presence or the absence of a non-linear summand in the Navier-Stokes equation. The low performance of computing machines at that time did not permit the full solution of this problem. Later, a similar problem was researched first by [4] and later by [5]. These authors presented the results of direct numerical modeling of large-scale structures in a periodic magnetic field, which reflected a change in the turbulence statistical parameters as a result of an imposed magnetic field influence. The contribution of these scientists in this area of expertise is determined by proving that the behavior of two- and three-dimensional structures varies substantially. A similar result was obtained by [6] in examining locally isotropic structures by the method of large eddies. Although the result obtained for the anisotropy invariant distribution and the Reynolds strength was discussed by several researchers, the findings on this matter cannot be considered conclusive because the force of the magnetic field is the determining factor for the change of quantitative indicators of invariants, which was not demonstrated by the author.

A generalization of a linear case researched by [2] and [3] is featured in publications by [7]. These researchers demonstrated a redistribution of the kinetic energy between velocity components, which indicated an inconsistency with a previously presented linear theory. In a nonlinear case, velocity components that are parallel and perpendicular to the magnetic field decay at various velocities, which is an apparent inconsistency with the earlier numerical experiments.

The process of the magnetic field influence on a developed turbulence was examined by [8], and demonstrated the possibility of using the quasi-stationary approximation for the solution of the second type problem and suggested to use quasi-linear approximations to solve the problem at  $Re_m = 20$ . One of the second type problem results were reported in [9], the modeling of a diminishing MHD turbulence by LES and DNS methods and demonstrated that the magnetic field at the initial time started to decay under the influence of the total kinetic energy. This effect is consistent with Joule dissipation. A similar picture of the decay was not reported by the authors because their main objective was the evaluation

the model adequacy for the LES and DNS methods. Accordingly, there was a justification of the modified dynamic Smagorinsky model for simulation of the temporal decaying magnetohydrodynamic turbulence.

The results of the third type of problem was presented by [10], and produced a detailed investigation of pseudospectral direct numerical simulation (DNS), with up to  $1024^3$  nodes, three-dimensional incompressible magnetohydrodynamic (MHD) turbulence, without the mean magnetic field. Study was carried out according to various statistical properties of the both decreasing and statistically steady MHD turbulence on the magnetic Prandtl number  $Pr_m$ , taken over in a wide range,  $0.01 \leq Pr_m \leq 10$ . Turbulent characteristics were obtained at a constant magnetic viscosity for different values of the kinetic viscosity.

This work is devoted to study of self-excitation of magnetic field and the motion of the conducting fluid at the same time taking into account acting forces. The idea is to specify in the phase space of initial conditions for the velocity field and magnetic field, which satisfy the condition of continuity. Given initial condition with the phase space is translated into physical space using a Fourier transform. The obtained of velocity field and magnetic field are used as initial conditions for the filtered MHD equations. Further is solved the unsteady three-dimensional equation of magnetohydrodynamics to simulate homogeneous MHD turbulence decay.

## 2 Problem

The numerical modeling of a homogeneous MHD turbulence decay based on the large eddy simulation method depending on the conductive properties of the incompressible fluid is reviewed.

The numerical modeling of the problem is performed based on solving non-stationary filtered magnetic hydrodynamics equations in conjunction with the continuity equation in the Cartesian coordinate system in a non-dimensional form:

$$\left\{ \begin{array}{l} \frac{\partial(\bar{u}_i)}{\partial t} + \frac{\partial(\bar{u}_i \bar{u}_j)}{\partial x_j} = -\frac{\partial(\bar{p})}{\partial x_i} + \frac{1}{Re} \frac{\partial}{\partial x_j} \left( \frac{\partial(\bar{u}_i)}{\partial x_j} \right) - \frac{\partial(\tau_{ij}^u)}{\partial x_j} + A \frac{\partial}{\partial x_j} (\bar{H}_i \bar{H}_j), \\ \frac{\partial(\bar{u}_j)}{\partial x_j} = 0, \\ \frac{\partial(\bar{H}_i)}{\partial t} + \frac{\partial(\bar{u}_j \bar{H}_i)}{\partial x_j} - \frac{\partial(\bar{H}_j \bar{u}_i)}{\partial x_j} = \frac{1}{Re_m} \frac{\partial}{\partial x_j} \left( \frac{\partial(\bar{H}_i)}{\partial x_j} \right) - \frac{\partial(\tau_{ij}^H)}{\partial x_j}, \\ \frac{\partial(\bar{H}_j)}{\partial x_j} = 0, \\ \tau_{ij}^u = ((\bar{u}_i \bar{u}_j) - (\bar{u}_i \bar{u}_j)) - ((\overline{H_i H_j}) - (\bar{H}_i \bar{H}_j)), \\ \tau_{ij}^H = ((\bar{u}_i \bar{H}_j) - (\bar{u}_i \bar{H}_j)) - ((\overline{H_i u_j}) - (\bar{H}_i \bar{u}_j)), \end{array} \right. \quad (1)$$

where  $\bar{u}_i$  ( $i = 1, 2, 3$ ) are the velocity components,  $\bar{H}_1, \bar{H}_2, \bar{H}_3$  are the magnetic field strength components,  $A = H^2/(4\pi\rho V^2) = \Pi/Re_m^2$  is the Alfvén number,  $H$  is the characteristic value of the magnetic field strength,  $V$  is the typical velocity,  $\Pi = (V_A L/\nu_m)^2$  is a dimensionless value (on which the value  $\Pi$  depends in the equation for  $\bar{H}_i$ ). If  $\Pi \ll 1$ , then  $\partial\bar{H}_i/\partial t = 0$ . The publication by [11] discussed in detail the physics of phenomena related to the ability to disregard the summand  $\partial\bar{H}_i/\partial t$ .  $(V_A)^2 = H^2/4\pi\rho$  is the Alfvén velocity,  $\bar{p} = p + \bar{H}^2 A/2$  is the full pressure,  $t$  is the time,  $Re = LV/\nu$  is the Reynolds number,  $Re_m = VL/\nu_m$  is the magnetic Reynolds number,  $L$  is the typical length,  $\nu$  is the kinematic viscosity coefficient,  $\nu_m$  is the magnetic viscosity coefficient,  $\rho$  is the density of electrically conducting incompressible fluid, and  $\tau_{ij}^u, \tau_{ij}^H$  is the subgrid-scale tensors responsible for small-scale structures to be modeled. To model a subgrid-scale tensor, a viscosity model is presented as  $\tau_{ij}^u = -2\nu_T \bar{S}_{ij}$ , where  $\nu_T = C_S \Delta^2 (2\bar{S}_{ij} \bar{S}_{ij})^{1/2}$  is the turbulent viscosity,  $\bar{S}_{ij} = (\partial\bar{u}_i/\partial x_j + \partial\bar{u}_j/\partial x_i)/2$  is the deformation velocity tensor value. To model a magnetic subgrid-scale tensor, a viscosity model is used:  $\tau_{ij}^H = -2\eta_t \bar{J}_{ij}$ , where  $\eta_t = D_S \Delta^2 (\bar{J}_{ij} \bar{J}_{ij})^{1/2}$  is the turbulent magnetic diffusion, the coefficients  $C_S, D_S$  are calculated for each determined time layer, and  $\bar{J}_{ij} = (\partial\bar{H}_i/\partial x_j - \partial\bar{H}_j/\partial x_i)/2$  is the magnetic rotation tensor.

Periodic boundary conditions are selected at all borders of the reviewed area of the velocity components and the magnetic field strength.

The initial values for each velocity component and strength are defined in the form of a function that depends on the wave numbers in the phase space:

$$u_i(k_i, 0) = k_i^{\frac{b-2}{2}} e^{-\frac{b}{4}\left(\frac{k_i}{k_{max}}\right)^2}; H_i(k_i, 0) = k_i^{\frac{b-2}{2}} e^{-\frac{b}{4}\left(\frac{k_i}{k_{max}}\right)^2},$$

where  $\bar{u}_i$  is the one-dimensional velocity spectrum,  $i = 1$  refers to the longitudinal spectrum,  $i = 2$  and  $i = 3$  refer to the transverse spectrum,  $\bar{H}_i$  is the one-dimensional magnetic field strength spectrum,  $m$  is the spectrum power, and  $k_1, k_2, k_3$  are the wave numbers.

For this problem we selected a variational parameter  $b$  and the wave number  $k_{max}$ , which determine the type of turbulence. For modeling homogeneous MHD turbulence can be set parameters  $k_{max}$  and  $b$ , which correspond to the experimental data [12].

### 3 Method for Calculating the Small-Scale Turbulence Coefficient

Along with the accepted calculated grid, a grid with twice the size of cells along each axis is used. The large grid number cell is indicated as  $p, g, r$  ( $p, g, r$  are the axes numbered  $x_1, x_2, x_3$ , respectively),  $p = 1, 2, 3, \dots, N_1/2$ ,  $g = 1, 2, 3, \dots, N_2/2$ , and  $r = 1, 2, 3, \dots, N_3/2$ . The cell with the number  $\alpha$  along axis  $x_1$  includes the cells of the initial grid with numbers  $n = 2p - 1$  and  $n = 2p$ , where  $n$  changes within the range from 1 to  $N_1$ . Similar to number  $g$ ,



for  $x_2$  determined cells with numbers  $m = 2g - 1$  and  $m = 2g$ ,  $q = 2r - 1$  and  $q = 2r$ . Therefore, one cell  $p, g, r$  of a large grid is the same as eight cells of the initial grid.

The average values  $u_1^2, u_2^2, u_3^2$  for the total volume of the calculated area of the liquid flow are marked  $\langle u_1 \rangle^2, \langle u_2 \rangle^2, \langle u_3 \rangle^2$ . These values can be calculated using smaller and larger calculation grids:

$$\langle u_i^2 \rangle = \frac{1}{N_1 N_2 N_3} \cdot \sum_{n=1}^{N_1} \sum_{m=1}^{N_2} \sum_{q=1}^{N_3} [(\bar{u}_i)^2 + (u_i')^2], \quad (2)$$

where  $(\bar{u}_i)^2 = \bar{u}_i \bar{u}_i$  and  $(u_i')^2 = \overline{u_i' \cdot u_i'}$ .

The subgrid-scale tensor for smaller cells is

$$\tau_{ij}^u = \overline{u_i' u_j'} = -2 \cdot C_S \cdot \Delta_s^2 \cdot (2 \cdot \bar{S}_{ij}^s \cdot \bar{S}_{ij}^s)^{\frac{1}{2}} \cdot \bar{S}_{ij}^s, \quad (3)$$

where  $\Delta_s = (\Delta_i \Delta_j \Delta_k)^{\frac{1}{3}}$  - is the width grid filter of the small cell.

The deformation velocity calculated in smaller cells is

$$\bar{S}_{ij}^s = \frac{1}{2} \left( \frac{\partial \bar{u}_i^s}{\partial x_j} + \frac{\partial \bar{u}_j^s}{\partial x_i} \right),$$

where  $n = \overline{1, N_1}$ ,  $m = \overline{1, N_2}$ ,  $q = \overline{1, N_3}$

By placing expression (3) into equation (2), we can obtain the average velocity value calculated in smaller cells:

$$\langle u_i^2 \rangle^s = \frac{1}{N_1 N_2 N_3} \cdot \sum_{n=1}^{N_1} \sum_{m=1}^{N_2} \sum_{q=1}^{N_3} \left[ (\bar{u}_i^s)^2 - 2 \cdot C_S \cdot \Delta_s^2 \cdot (2 \cdot S_{ij}^s \cdot S_{ij}^s)^{\frac{1}{2}} S_{ij}^s \right]. \quad (4)$$

The average velocity calculated in larger cells is

$$\langle u_i^2 \rangle^l = \frac{8}{N_1 N_2 N_3} \cdot \sum_{p=1}^{N_1/2} \sum_{g=1}^{N_2/2} \sum_{r=1}^{N_3/2} \left[ (\bar{u}_i^l)^2 - 2 \cdot C_S \cdot \Delta_l^2 \cdot (2 \cdot S_{ij}^l \cdot S_{ij}^l)^{\frac{1}{2}} S_{ij}^l \right]. \quad (5)$$

where  $\Delta_l = (\Delta_i \Delta_j \Delta_k)^{\frac{1}{3}}$  - is the width grid filter of the large cell,  $\Delta_l = 2 \cdot \Delta_s$ .

The deformation velocity calculated in larger cells is

$$\bar{S}_{ij}^l = \frac{1}{2} \left( \frac{\partial \bar{u}_i^l}{\partial x_j} + \frac{\partial \bar{u}_j^l}{\partial x_i} \right),$$

where  $p = 1, 2, 3, \dots, \frac{N_1}{2}$ ;  $g = 1, 2, 3, \dots, \frac{N_2}{2}$ ;  $r = 1, 2, 3, \dots, \frac{N_3}{2}$ .

$$\bar{u}_i^l(p, g, r) = \frac{1}{8} \left[ \begin{array}{l} \bar{u}_i^s(2p-1, 2g-1, 2r-1) + \bar{u}_i^s(2p-1, 2g, 2r-1) + \\ + \bar{u}_i^s(2p-1, 2g, 2r) + \bar{u}_i^s(2p-1, 2g-1, 2r) + \\ + \bar{u}_i^s(2p, 2g-1, 2r-1) + \bar{u}_i^s(2p, 2g, 2r-1) + \\ + \bar{u}_i^s(2p, 2g, 2r) + \bar{u}_i^s(2p, 2g-1, 2r) \end{array} \right].$$

We introduce the following notation:

$$F^u = (\langle \bar{u}_1^2 \rangle^s + \langle \bar{u}_2^2 \rangle^s + \langle \bar{u}_3^2 \rangle^s - \langle \bar{u}_1^2 \rangle^l - \langle \bar{u}_2^2 \rangle^l - \langle \bar{u}_3^2 \rangle^l)^2.$$

From equations (4) and (5), we can conclude

$$F^u = (Z^u - Y^u \cdot C_S)^2,$$

where

$$\begin{aligned} Z^u &= \frac{1}{N_1 N_2 N_3} \cdot \sum_{n=1}^{N_1} \sum_{m=1}^{N_2} \sum_{q=1}^{N_3} (\bar{u}_i^2)^s - \frac{8}{N_1 N_2 N_3} \cdot \sum_{p=1}^{N_1/2} \sum_{g=1}^{N_2/2} \sum_{r=1}^{N_3/2} (\bar{u}_i^2)^l, \\ Y^u &= \frac{1}{N_1 N_2 N_3} \cdot \sum_{n=1}^{N_1} \sum_{m=1}^{N_2} \sum_{q=1}^{N_3} (-2 (\Delta_s)^2 (2S_{ij}^s S_{ij}^s)^{\frac{1}{2}} S_{ij}^s) - \\ &\quad - \frac{8}{N_1 N_2 N_3} \cdot \sum_{p=1}^{N_1/2} \sum_{g=1}^{N_2/2} \sum_{r=1}^{N_3/2} (-2 (\Delta_l)^2 (2S_{ij}^l S_{ij}^l)^{\frac{1}{2}} S_{ij}^l). \end{aligned}$$

The condition for achieving the minimum is

$$\frac{\partial F^u}{\partial C_S} = -2 (Z^u - Y^u \cdot C_S) \cdot Y^u = 0.$$

Thus,  $Z^u - Y^u \cdot C_S = 0$ .

At a certain time layer  $T_{step}$  the empirical coefficient of viscosity model is calculated by the following formula:  $C_S = Z^u / Y^u$ , where  $T_{step} = 10 \cdot \tau$ ,  $\tau$ -time step.

#### 4 Method for Calculating the Small-Scale Magnetic Field

Here is used the same grid, which was used to calculate the small-scale turbulence coefficient, which deals with the grid twice the size of cells along each axis.

The average values of magnetic field strength  $H_1^2$ ,  $H_2^2$ ,  $H_3^2$  for the total volume of the calculated area of the liquid flow are marked  $\langle H_1 \rangle^2$ ,  $\langle H_2 \rangle^2$ ,  $\langle H_3 \rangle^2$ . These values can be calculated using smaller and larger calculation grids:

$$\langle H_i^2 \rangle = \frac{1}{N_1 N_2 N_3} \cdot \sum_{n=1}^{N_1} \sum_{m=1}^{N_2} \sum_{q=1}^{N_3} [(\bar{H}_i)^2 + (H'_i)^2], \quad (6)$$

where  $(\bar{H}_i)^2 = \bar{H}_i \bar{H}_i$  and  $(H'_i)^2 = \overline{H'_i \cdot H'_i}$ .

The magnetic subgrid-scale tensor for smaller cells is

$$\tau_{ij}^H = \overline{H'_i H'_j} = -2 \cdot D_S \cdot \Delta_s^2 \cdot (2 \cdot \bar{J}_{ij}^s \cdot \bar{J}_{ij}^s)^{\frac{1}{2}} \cdot \bar{J}_{ij}^s. \quad (7)$$

The magnetic rotation tensor calculated in smaller cells is

$$\bar{J}_{ij}^s = \frac{1}{2} \left( \frac{\partial \bar{H}_i^s}{\partial x_j} - \frac{\partial \bar{H}_j^s}{\partial x_i} \right),$$

where  $n = \overline{1, N_1}$ ,  $m = \overline{1, N_2}$ ,  $q = \overline{1, N_3}$

By placing expression (7) into equation (6), we can obtain the average velocity value calculated in smaller cells:

$$\langle H_i^2 \rangle^s = \frac{1}{N_1 N_2 N_3} \cdot \sum_{n=1}^{N_1} \sum_{m=1}^{N_2} \sum_{q=1}^{N_3} \left[ (\overline{H}_i^s)^2 - 2 \cdot D_S \cdot \Delta_s^2 \cdot (2 \cdot J_{ij}^s \cdot J_{ij}^s)^{\frac{1}{2}} J_{ij}^s \right]. \quad (8)$$

The average value of magnetic field strength calculated in larger cells is

$$\langle H_i^2 \rangle^l = \frac{8}{N_1 N_2 N_3} \cdot \sum_{p=1}^{N_1/2} \sum_{g=1}^{N_2/2} \sum_{r=1}^{N_3/2} \left[ (\overline{H}_i^l)^2 - 2 \cdot D_S \cdot \Delta_l^2 \cdot (2 \cdot J_{ij}^l \cdot J_{ij}^l)^{\frac{1}{2}} J_{ij}^l \right]. \quad (9)$$

The magnetic rotation tensor calculated in larger cells is

$$\overline{J}_{ij}^l = \frac{1}{2} \left( \frac{\partial \overline{H}_i^l}{\partial x_j} - \frac{\partial \overline{H}_j^l}{\partial x_i} \right),$$

where  $p = 1, 2, 3, \dots, N_1/2$ ;  $g = 1, 2, 3, \dots, N_2/2$ ;  $r = 1, 2, 3, \dots, N_3/2$ .

$$\overline{H}_i^l(p, g, r) = \frac{1}{8} \left[ \begin{array}{l} \overline{H}_i^s(2p-1, 2g-1, 2r-1) + \overline{H}_i^s(2p-1, 2g, 2r-1) + \\ + \overline{H}_i^s(2p-1, 2g, 2r) + \overline{H}_i^s(2p-1, 2g-1, 2r) + \\ + \overline{H}_i^s(2p, 2g-1, 2r-1) + \overline{H}_i^s(2p, 2g, 2r-1) + \\ + \overline{H}_i^s(2p, 2g, 2r) + \overline{H}_i^s(2p, 2g-1, 2r) \end{array} \right].$$

We introduce the following notation:

$$F^H = \left( \langle \overline{H}_1^2 \rangle^s + \langle \overline{H}_2^2 \rangle^s + \langle \overline{H}_3^2 \rangle^s - \langle \overline{H}_1^2 \rangle^l - \langle \overline{H}_2^2 \rangle^l - \langle \overline{H}_3^2 \rangle^l \right)^2.$$

From equations (8) and (9), we can conclude

$$F^H = (Z^H - Y^H \cdot D_S)^2,$$

where

$$Z^H = \frac{1}{N_1 N_2 N_3} \cdot \sum_{n=1}^{N_1} \sum_{m=1}^{N_2} \sum_{q=1}^{N_3} (\overline{H}_i^2)^s - \frac{8}{N_1 N_2 N_3} \cdot \sum_{p=1}^{N_1/2} \sum_{g=1}^{N_2/2} \sum_{r=1}^{N_3/2} (\overline{H}_i^2)^l,$$

$$Y^H = \frac{1}{N_1 N_2 N_3} \cdot \sum_{n=1}^{N_1} \sum_{m=1}^{N_2} \sum_{q=1}^{N_3} (-2 (\Delta_s)^2 (2 J_{ij}^s J_{ij}^s)^{\frac{1}{2}} J_{ij}^s) - \\ - \frac{8}{N_1 N_2 N_3} \cdot \sum_{p=1}^{N_1/2} \sum_{g=1}^{N_2/2} \sum_{r=1}^{N_3/2} (-2 (\Delta_l)^2 (2 J_{ij}^l J_{ij}^l)^{\frac{1}{2}} J_{ij}^l).$$

The condition for achieving the minimum is

$$\frac{\partial F^H}{\partial D_S} = -2(Z^H - Y^H \cdot D_S) \cdot Y^H = 0.$$

Hence,  $Z^H - Y^H \cdot D_S = 0$ .

Thus, the empirical coefficient of viscosity model for magnetic field at a certain time step  $T_{step}$  assumes the following form:  $D_S = Z^H / Y^H$ .

## 5 Numerical Method

To solve the problem of homogeneous incompressible MHD turbulence, a scheme of splitting by physical parameters is used:

- I.  $(\mathbf{u}^* - \mathbf{u}^n) / \tau = -(\mathbf{u}^n \nabla) \mathbf{u}^* + A (\mathbf{H}^n \nabla) \mathbf{H}^n + (1/Re) (\Delta \mathbf{u}^*) - \nabla \tau^u$ ,
- II.  $\Delta p = \nabla \mathbf{u}^* / \tau$ ,
- III.  $(\mathbf{u}^{n+1} - \mathbf{u}^*) / \tau = -\nabla p$ .
- IV.  $(\mathbf{H}^{n+1} - \mathbf{H}^n) / \tau = -rot(\mathbf{u}^{n+1} \times \mathbf{H}^{n+1}) + \nu_m \Delta \mathbf{H}^{n+1} - \nabla \tau^H$

The following physical interpretation of the splitting diagram is suggested. During the first stage, the Navier-Stokes equation is solved without the pressure consideration. For the approximation of convective and diffusion equation members, a compact scheme of an increased order of accuracy is used [13]. During the second stage, the Poisson equation is solved, which is obtained from the continuity equation by considering the velocity fields of the first stage. For the three-dimensional Poisson equation, an original solution algorithm was developed – a spectral transform in combination with the matrix run. During the third stage, the obtained pressure field is used to recalculate the final velocity field. During the fourth stage, the obtained velocity field is used to solve the equation to obtain the components of the magnetic field strength, which are included in the initial equation.

## 6 Numerical Modeling Results

Numerical model allows to describe the homogeneous magnetohydrodynamic turbulence decay based on large eddy simulation. For this task, the kinematic viscosity  $\nu = 10^{-4}$  was taken constant and the magnetic viscosity were set in the range of  $\nu_m = 10^{-3} \div 10^{-4}$ . The characteristic values of the velocity, length, magnetic field strength were taken equal to:  $U_{CH} = 1$ ,  $L_{CH} = 1$ ,  $H_{CH} = 1$  respectively. Reynolds number is  $Re = 10^4$ , the magnetic Reynolds number varied depending on the magnetic viscosity coefficient. The Alfvén number characterizing the motion of conductive fluid for various numbers of magnetic Reynolds:

$A = Ha^2/Re_m$ , where Hartmann number is  $Ha = 1$ . For the calculations used grid size  $128 \times 128 \times 128$ . The time step was taken equal  $\Delta\tau = 0.001$ .

As result of simulation at different magnetic Reynolds numbers were obtained the following turbulence characteristics: kinetic energy, magnetic energy, integral scale longitudinal correlation functions.

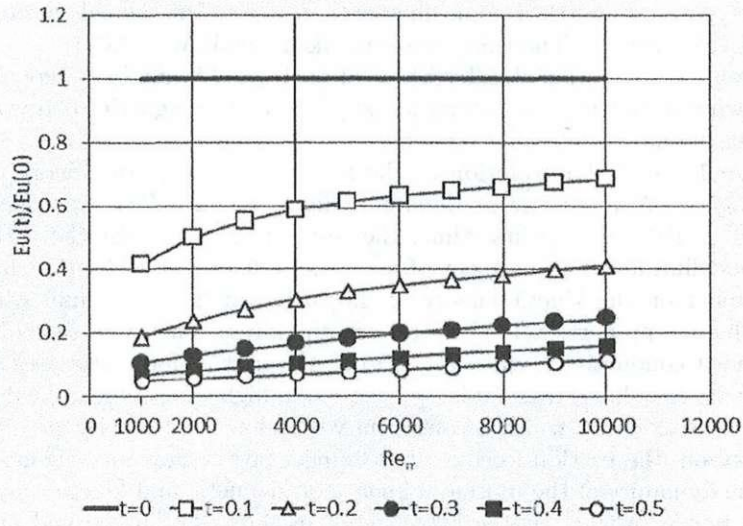
Figure 1 shows the evolution of the kinetic and magnetic energy changes depending on  $Re_m$  number at different points in time.  $Re_m$  was selected in range  $10^3 \div 10^4$ . For the first time, the result is obtained for the turbulence decay modeling under the impact of a magnetic field caused by the change in  $Re_m$  number on the kinetic energy of the turbulent flow of a fluid with various conductive properties. It is easily seen the kinetic energy in case of a high environment conductivity, when  $Re_m = 10^3$ , the friction force increases and the flow velocity is reduced more quickly in case of a high environment conductivity than when  $Re_m = 10^4$ , which is consistent with a low conductivity environment, in this option, the friction force has less impact on the flow rate. Thus, 1 illustrates the dynamics of the mutual influence of magnetic and kinetic energies at different points in time: at the initial point in time, the kinetic and magnetic energies are defined identically; at the next point when the fluid with a higher conductivity is studied, the turbulence decay occurs faster than in case where  $Re_m$  starts to increase, which determines the fluid with a lesser conductivity. When value  $Re_m = 10000$ , the turbulence decay virtually corresponds to the case of an isotropic turbulence decay, as per Abdibekov and Zhakebayev [14].

According to semi-empirical theory of turbulence integral scale should grow with time. The results presented in Figure 2 illustrates the effect of magnetic viscosity on the internal structure of the MHD turbulence. Variation of the coefficient of magnetic viscosity leads to a proportional change in the integral scale. Figure 2 shows that the size of large eddies rapidly increases at small number of magnetic Reynolds  $Re_m = 10^3$ , than in the case, when  $Re_m = 10^4$  which leads to fast energy dissipation.

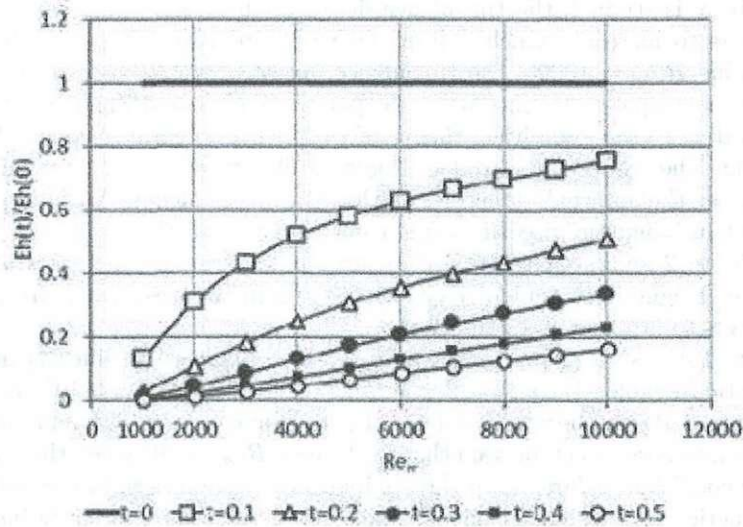
Figure 3 shows the change in the micro scale - calculated at different numbers of magnetic Reynolds 1)  $Re_m = 10^3$ ; 2)  $Re_m = 2 \cdot 10^3$ ; 3)  $Re_m = 5 \cdot 10^3$ ; 4)  $Re_m = 10^4$ . Figure 3 shows the change of the Taylor microscale at different magnetic Reynolds numbers. It can be seen that in the case  $Re_m = 10^3$  when the magnetic viscosity coefficient is large then the dissipation rate increases. In the case when the magnetic viscosity coefficient is smaller then the scale gradually increases, and the small scale structure of the turbulence tends to slowly isotropy. This also indicates that with small numbers  $Re_m$  the decay of isotropic turbulence occurs faster than in the case when  $Re_m$  is high.

Figure 4 shows the changes of the longitudinal correlation function calculated at  $Re_m = 10^3$  and  $Re_m = 10^4$ . These illustrations also show that there are an influence of the magnetic field on the isotropic turbulence decay, as these figures are fixed the result of changes in the correlation functions at different  $Re_m$ .

The correlation function is expressed the average by volume the correlation ratio between the components of the velocity at various points, the farther points are located between the various components of the velocity, the smaller should



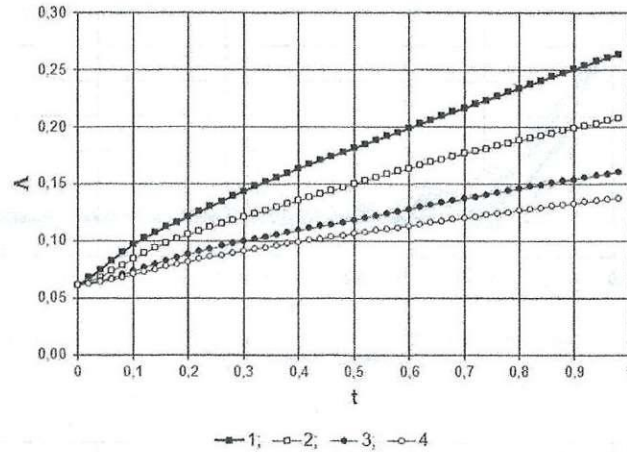
(a)



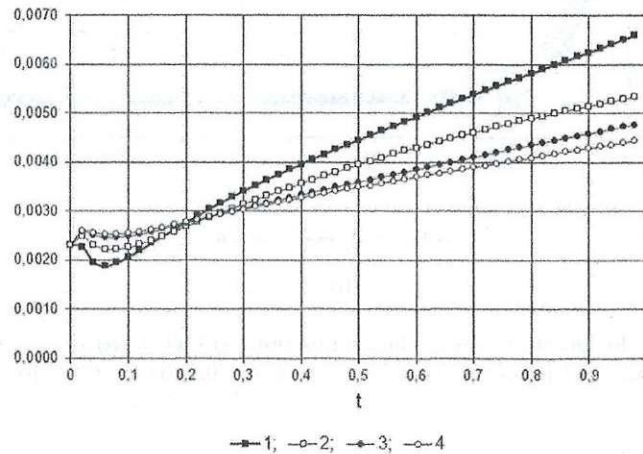
(b)

Fig. 1. Change of the kinetic (a) and magnetic (b) energies depending on the  $Re_m$  number at different points in time

be the correlation coefficients, i.e. they should be close to zero. Figure 4a shows the change in the longitudinal correlation function  $f(r)$  in time and calculated at  $Re = 10^4$ ,  $Re_m = 10^3$ . It is seen that with increasing value  $r$  of the function



**Fig. 2.** Change of the integral turbulence scale calculated at different magnetic Reynolds numbers: 1)  $Re_m = 10^3$ ; 2)  $Re_m = 2 \cdot 10^3$ ; 3)  $Re_m = 5 \cdot 10^3$ ; 4)  $Re_m = 10^4$



**Fig. 3.** Change of Taylor-scale calculated at different magnetic Reynolds numbers: 1)  $Re_m = 10^3$ ; 2)  $Re_m = 2 \cdot 10^3$ ; 3)  $Re_m = 5 \cdot 10^3$ ; 4)  $Re_m = 10^4$

tends to zero. Character of the correlations change corresponds to the change of the correlation functions given in [14].

From the figures it is seen that in the case of high medium conductivity at  $Re_m = 10^3$  the frictional force increases and the flow rate is reduced faster than, at  $Re_m = 10^4$ , that corresponds to the low conductivity of the medium, in this version, the frictional force have minimal impact on the flow velocity. Based on the study of the results determined that the first part of the turbulent kinetic energy is used for turbulent mixing, the second part - at creating magnetic field and the third part - on the forces of resistance between the components of the velocity and magnetic tension.

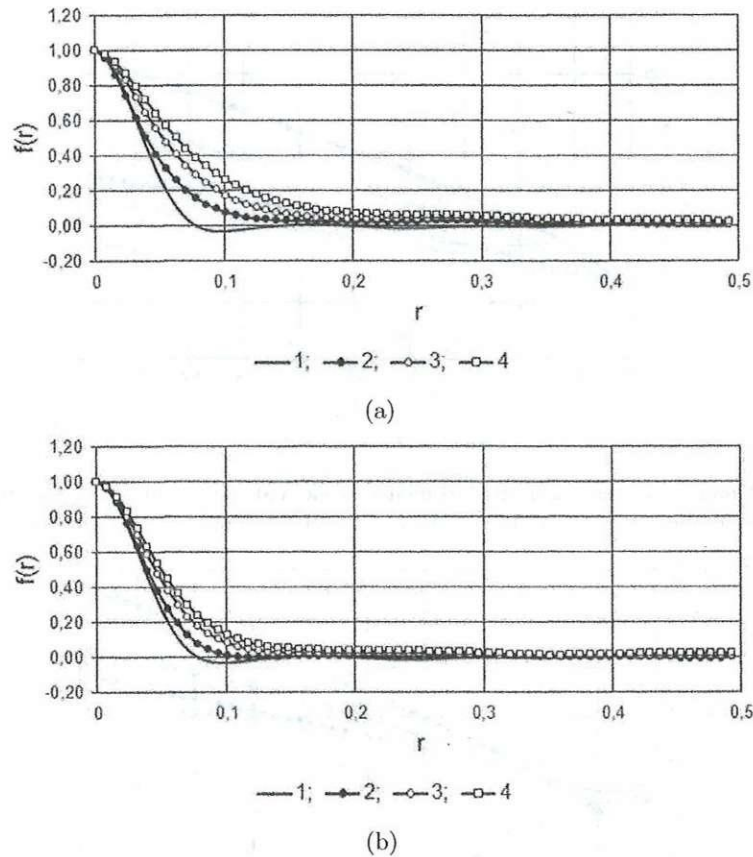


Fig. 4. Change the longitudinal correlation function  $f(r)$  when (a)  $Re_m = 10^3$  and (b)  $Re_m = 10^4$  at different points in time: 1)  $t = 0$ ; 2)  $t = 0.2$ ; 3)  $t = 0.3$ ; 4)  $t = 0.5$

## 7 Conclusions

Based on the method large-eddy simulation was produced the numerical modelling of influence magnetic viscosity to decay of homogeneous magnetohydrodynamic turbulence, analyzing simulation results it is possible to make the following conclusion: the magnetic viscosity of the flow has a significant influence on the MHD turbulence, and therefore can be used for process control in the preparation semiconductor structures of single crystals. Obtained results allow sufficiently accurately calculate the change characteristics of homogeneous magnetohydrodynamic turbulence over time at large magnetic Reynolds numbers. Thus, the numerical algorithm was developed for solving unsteady three-dimensional magnetohydrodynamic equations, for modeling MHD turbulence decay at different magnetic Reynolds numbers. Physical processes and phenomena of homogeneous magnetohydrodynamic turbulence identified in the numerical simulation. The



proposed method can be used to solve the MHD turbulence without significant changes.

## References

1. Batchelor, G.K.: On the spontaneous magnetic field in a conducting liquid in turbulent motion. *Proc. Roy. Soc. A* **201**(16), 405–416 (1950)
2. Schumann, U.: Numerical simulation of the transition from three- to two-dimensional turbulence under a uniform magnetic field. *J. Fluid Mech.* **74**, 31–58 (1976)
3. Moffatt, H.K.: On the suppression of turbulence by a uniform magnetic field. *J. Fluid Mech.* **28**, 571–592 (1967)
4. Hossain, M.: Inverse energy cascades in three dimensional turbulence. *Phys. Fluids B*. **3**(2), 511–514 (1991)
5. Zikanov, O., Thess, A.: Direct numerical simulation of forced MHD turbulence at low magnetic Reynolds number. *J. Fluid Mech.* **358**(1), 299–333 (1998)
6. Vorobev, A., Zikanov, O., Davidson, P.A., Knaepen, B.: Anisotropy of magnetohydrodynamic turbulence at low magnetic Reynolds number. *Phys. Fluid 17* (2005)
7. Burattini, P., Zikanov, O., Knaepen, B.: Decay of magnetohydrodynamic turbulence at low magnetic Reynolds number. *J. Fluid Mech.* **657**, 502–538 (2010)
8. Knaepen, B., Kassinos, S., Carati, D.: Magnetohydrodynamic turbulence at moderate magnetic Reynolds number. *J. Fluid Mech.* **513**(3), 199–220 (2004)
9. Knaepen, B., Moin, P.: Large-eddy simulation of conductive flows at low magnetic Reynolds number. *Physics of Fluids* **16**, 1255–1261 (2004)
10. Sahoo, G., Perlekar, P., Pandit, R.: Systematics of the magnetic-Prandtl-number dependence of homogeneous, isotropic magnetohydrodynamic turbulence. *New J. Phys.* **13**, 1367–2630 (2011)
11. Ievlev, V.M.: The method of fractional steps for solution of problems of mathematical physics. *Science Nauka, Moscow* (1975)
12. Sirovich, L., Smith, L., Yakhot, V.: Energy spectrum of homogeneous and isotropic turbulence in far dissipation range. *Physical Review Letters* **72**(3), 344–347 (1994)
13. Zhumagulov, B., Abdibekov, U., Zhakebaev, D., Zhubat, K.: Modelling isotropic turbulence decay based on the LES. *Mathematical modelling* **25**(1), 18–32 (2013)
14. Abdibekov, U.S., Zhakebaev, D.B.: Modelling of the decay of isotropic turbulence by the LES. *J. Phys.: Conf. Ser.* 318 (2011)